SYNTHESIS AND CHARACTERIZATION OF A MACROCYCLE CONTAINING ASPARTIC ACID

by

Carl Berghult

Submitted in partial fulfillment of the

requirements for Departmental Honors in

the Department of Chemistry and Biochemistry

Texas Christian University

Fort Worth, Texas

May 8, 2023

SYNTHESIS AND CHARACTERIZATION OF A MACROCYCLE CONTAINING ASPARTIC ACID

Project Approved:

Supervising Professor: Eric Simanek, Ph.D.

Department of Chemistry and Biochemistry

David Minter, Ph.D.

Department of Chemistry and Biochemistry

Matthew Hale, Ph.D.

Department of Biology

Abstract

The long-term motivation for exploring macrocycles—molecules wherein at least 12 of the atoms are arranged in a ring—is to be able to produce drugs that can interfere with specific protein-protein interactions within cells. Many diseases involve abnormal cellular protein-protein interactions that have the potential to be disrupted by macrocycles that would improve the physical manifestation of disease. The molecule described in this thesis incorporates the amino acid aspartic acid. Aspartic acid is particularly intriguing due to the ionizable carboxylic acid group on its side chain and its ability to hydrogen bond. This potential offers the possibility of previously unreported three-dimensional shapes and dynamic behavior for this family of molecules.

The macrocycle was synthesized in three steps. First, cyanuric chloride was substituted with BOC-hydrazine dropwise in THF under basic conditions while being carefully monitored by thin layer chromatography (TLC) to prevent excess substitution. In the same reaction vessel, Boc-protected aspartic acid was added under basic conditions and monitored by TLC. To complete the first step, dimethyl amine was subsequently added also to the same vessel. Following extraction and chromatography, the first intermediate was obtained. In the second step, this intermediate was reacted with an amino acetal to form the monomer. Again, an extraction was performed followed by chromatography. The third synthetic step was a reaction with acid to produce the dimeric macrocycle.

Characterization of the macrocycle was accomplished using various methods. Both one-dimensional and two-dimensional proton NMR spectroscopy confirmed the structures of the macrocycle and the intermediates. Clues to the three-dimensional structure were obtained using two-dimensional ROESY and variable temperature NMR experiments as well as and data from related molecules.

Acknowledgements

I would like to thank everyone involved with guiding me through the process and helping me achieve a long-time goal of mine to write an honors thesis. This would not be possible without the support and advice from the great professors around me. I would like to specifically thank Dr. Eric Simanek for his continued support and mentorship through the process. Thank you to Dr. Matt Hale and Dr. David Minter for serving on my honors committee. To my friends and family, thank you for always having my back and being my support staff. This work is truly a reflection of the great people I have surrounding me. Finally, I would like to thank the John V. Roach Honors College and Texas Christian University for providing the resources and facilities to make this a reality. Go frogs!

TABLE OF CONTENTS

TERMINOLOGY AND ABBREVIATIONS

Abbreviation	Full Term
BOC	*tert*-butyloxycarbonyl
C	carbon
COSY	correlation spectroscopy
DCM	dichloromethane
DIPEA	diisopropylethylamine
DMA	dimethylamine
DMSO	dimethyl sulfoxide
EDC	1-ethyl-3-(3-dimethylaminopropyl) carbodiimide
H	hydrogen
HOBT	hydroxybenzotriazole
MeOH	Methanol
N	Nitrogen
NMR	nuclear magnetic resonance
ROESY	rotating-frame Overhauser effect spectroscopy
TLC	thin-layer chromatography
THF	tetrahydrofuran

FIGURES AND SCHEMES

Introduction

Many drugs on the market derive from nature or are inspired by natural products.[1] Many of these drugs are large macrocycles that display variable side chains to interact with their targets. Oftentimes, this involves interfering with protein-protein interactions within the cell or blocking sites that proteins recognize.[2] Traditionally, however, the pharmaceutical industry has explored small molecule drugs. These drugs work by a different therapeutic paradigm. They block enzyme active sites.[3] Now, the pharmaceutical industry is increasingly interested in macrocycles. The rules for designing small molecule and macrocycle drugs differ greatly.[4]

One of the key design criteria for macrocycles—in addition to developing ways to easily swap out various functional groups and atoms to promote binding—is to allow for dynamic motion. Macrocycles require the unique ability to fold and unfold in response to various environments.[5] That is, a macrocycle typically will open broadly to expose a large surface area and many hydrophilic groups in order to bind to its protein target. But if this target is inside a cell or if the drug is to be taken orally, the macrocycle must also fold up to present a hydrophobic exterior to pass across cell membranes. [6] The molecule's ability to adopt different conformations ensures that it will be at least partially soluble in an array of physiologically relevant environments.

The macrocycles being explored in the Simanek Lab are dimers comprising an aromatic triazine ring that is substituted easily. Critical groups include a protected hydrazine and an acetal.[5] When these groups are exposed to acid, they react to form the macrocycle. The acetal is connected by an amino acid. Given the large number of amino acids that are available, this design meets some of

the expectations set forth by current methods in drug development. There is also a third position on the ring that can be substituted. As a result, there is significant freedom in molecular design. Considering the choice of 1) the final amine substitution, 2) the amino acid selection, and 3) the length of the acetal which controls ring size, a plethora of possibilities exist.[7] The ease of substitution and numerous possibilities for swapping out functional groups is exactly why macrocyclic molecules are important for future drug design. Many efforts in the lab focus on incorporating different amino acids into the macrocycle.

The macrocycle synthesized here contains aspartic acid. The choice of amino acid is important in the design criteria. Amino acids are distributed differently within proteins both in relative amounts and locations.[8] Chart 1 shows the frequency with which each amino acid appears globally and on the surface of a globular proteins. If all were equal, there would be no difference where each of the amino acids appear on proteins. With 20 amino acids, we would expect 5% for each entry. However, the difference in functional groups on each side chain determines whether they will be found on the surface or inside globular proteins. Hydrophilic amino acids tend to appear on the surface of proteins whereas hydrophobic amino acids are observed as being globally distributed. Interestingly, amino acids with aromatic side chains find themselves with a fairly even distribution globally and on the surface of proteins.

My research focuses on aspartic acid. It was chosen due to its hydrophilic nature. It is incorporated into proteins at 5%, the statistical average. However, the carboxylic acid functional group causes the amino acid to appear frequently on the surface of proteins which could be important for disrupting protein-protein interactions within the cell.

Chart 1. The distribution of amino acids across 10,000 globular proteins showing residuals at the surface (blue) and on the interior (orange).

Random, equivalent enrichment would yield a 5% value for both bars. (Reproduced from Reference 8).

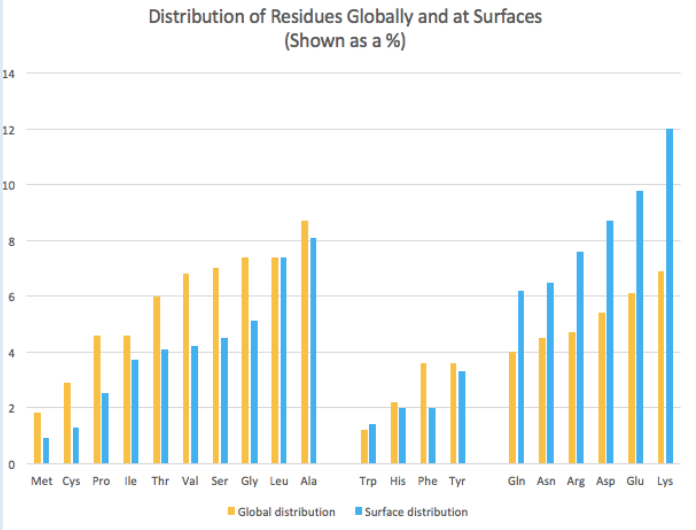

Not only do the amino acid distributions within proteins vary, but also the amino acids that exist at protein-protein interfaces vary as well. This knowledge is important as we look to design macrocycles that interfere at these sites. Chart 2 shows this distribution and the amounts of energy these amino acids contribute to binding. If all amino acids were the same, then there would be an even distribution of amino acids at each binding interface with each appearing at 100%. Clearly, that is not what is observed. Aspartic acid is enriched slightly at interfaces—and importantly—contributes significantly to tight binding interactions.

Chart 2. The percent enrichment at sites of protein-protein interaction (green) and the percentage that contribute at least 2 kcal/mol to binding energy.

If an amino acid appeared on the surface 5% of the time and appeared at a binding hot-spot 5% of the time, a value of 100% would be reported for both. (Reproduced from Reference 8).

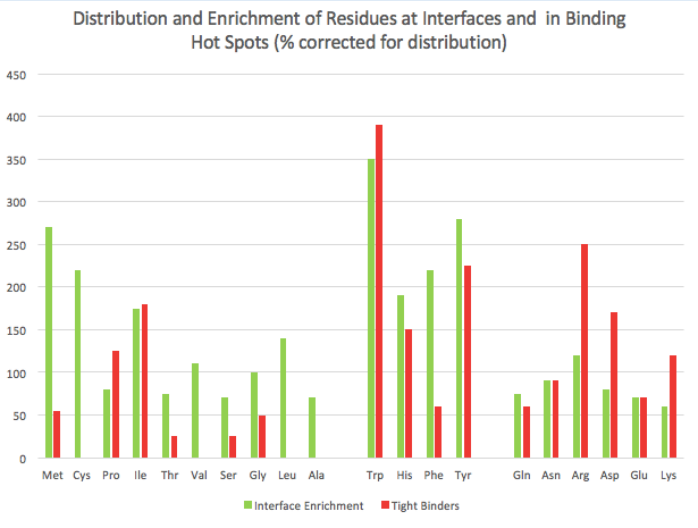

Aspartic acid is one of a few amino acids that exists in a charged state at physiological pH. It has the relatively unique capability of adapting to different solvents and cellular environments by altering its protonation state. When the molecule is in a low pH environment like the stomach it will exist in its protonated, more hydrophobic form. At high pH like the blood stream or within cells, it is more hydrophilic because it is deprotonated. The ability to change protonation states and thus charge further contributes to the molecule's dynamic nature.[9] Aspartic acid is closely related to glutamic acid with the exclusion of one carbon on its side chain. The shorter side chain means that binding interactions will occur closer to the macrocyclic ring structure. Many parallels can be drawn between aspartic acid and glutamic acid, but their relationship in macrocyclic compounds is unknown. Making these molecules and examining their physical properties is a first step towards understanding these differences.

Experimental

D-Acid. While continuously stirring, cyanuric chloride (0.509 g, 2.74 mmol) was added as a solid and dissolved in 5 mL of THF that was cooled to 0 °C. The temperature was maintained while a 5 mL solution of BOC-hydrazine (0.354 g, 2.74 mmol) in THF (0.5 M) was added dropwise. After the addition was complete, the solution turned a bright yellow color. Next, 1.08 mL of 5 M NaOH (2.74 mmol) was added via pipette. After 3-hour, thin layer chromatography (10% methanol in dichloromethane) showed a single product was observed under short wave UV irradiation ($R_f = 0.6$) and using ninhydrin (yellow spot). The ice bath was then removed, and the solution was allowed to stir and slowly warm to room temperature. A solution of aspartate (t-butyl protected) (0.991 g, 5.42 mmol) was added neat while at room temperature. The reaction mixture was at a pH of 7.5 after this addition of the amino acid. The solution continued with a bright yellow color and dulled a bit after the addition. After 3 h, thin layer chromatography showed the starting material ($R_f = 0.7$) disappeared and a new spot at $R_f = 0.1$ appeared. Dimethylamine (0.616 g, 5.42mmol) was then added dropwise (40% DMA in 60% H_20). Following the addition, the pH was measured to be 8. The reaction was stirred for another 3 h at room temperature. This layer chromatography showed the appearance of a new spot at $R_f = 0.3$. The solution was diluted with 150 mL of brine and extracted with three 50 mL additions of ethyl acetate. The organic layer was dried using $MgSO_4$ and excess solvent removed via rotary evaporation. Column chromatography was prepared in (10% MeOH: DCM) and the reaction yielded 0.539 g pure product (51.1%).

^{1}H NMR (DMSO-d_6, 400 MHz): δ 12.76 – 12.70 (s, 1H), 8.26 – 8.08 (d, 1H), 6.92 – 6.67 (m, 1H), 4.73 – 4.61 (m, 1H), 3.06 – 3.02 (d, 6H), 2.75 – 2.61 (m, 1H), 1.40 – 1.30 (m, 25H)

Monomer D. With continuous stirring, the D-acid product (0.230 g, 0.5227 mmol), diethoxypropyl amine (0.0768 g, 0.5227 mmol), and HOBT (0.096 g, 0.627 mmol) were dissolved in 1.5 mL DCM at room temperature. Following the addition, DIPEA (0.168 g, 1.31 mmol) and EDC.HCl (0.1204 g, 0.627 mmol) were added neat. After 3 hours, thin layer chromatography (5% methanol in dichloromethane) confirmed the single spot starting material (R_f = 0.3) evolved into multiple new spots under UV radiation at an R_f of 0.6 in 5% MeOH in DCM. The reaction mixture was dissolved in 50 mL of ethyl acetate and washed with water (3x50 mL). Column Chromatography was then performed with 2.5% chloroform in DCM. A single fraction containing a single spot via TLC was isolated and analyzed using NMR data.
^{1}H NMR ($CDCl_3$, 400 MHz): δ 6.96 (s, 1H), 6.44 (m, 1H), 5.91 (m, 1H), 4.88 (m, 1H), 4.51 (s, 1H), 3.64 – 3.62 (m, 2H), 3.60 – 3.49 (m, 2H), 3.47 – 3.45 (m, 2H), 3.07 (d, 6H), 2.96 – 2.90 (m, 1H), 1.82 – 1.79 (d, 1H), 1.61 (s, 1H), 1.47 – 1.40 (m, 25H), 1.21 – 1.15 (m, 6H).

Macrocycle D-D. Monomer D (10 mg) was dissolved in 1 mL of DCM in a vial with stir bar added. TFA (1 mL) was added dropwise to the reaction vial via pipette. The vial cap was removed for slow evaporation. Evaporation occurred over the course of 7 days. After full evaporation macrocyclization was confirmed via NMR.
^{1}H NMR (DMSO-d_6, 400 MHz): δ 12.45 (s, 1H), 12.16 (s, 1H), 11.73 (s, 1H), 9.05 (s, 1H), 8.07 (s, 1H), 7.46 – 7.41 (d,2H), 4.68 (s, 1H), 4.02 (s, 1H), 3.31 – 3.25 (m, 1H), 3.14 – 3.11 (m, 12H), 2.86 – 2.78 (m, 4H), 2.59 (m, 2H).

Results and Discussion

Part 1. The D-D Macrocycle.

Figure 1 shows the **D-D Macrocycle**. The cyclical nature of the target compound is evident. The ring contains 24 atoms. The dimeric nature is shown as are the constituent parts including the triply substituted triazine ring, the aspartic acid designated with the labels a and b, the acetal designated with A, B and C, the dimethyl amine auxiliary group labeled M1 and M2, and the hydrazone bonds that are created when the macrocycle forms.

Figure 1. Macrocycle D-D and labels.

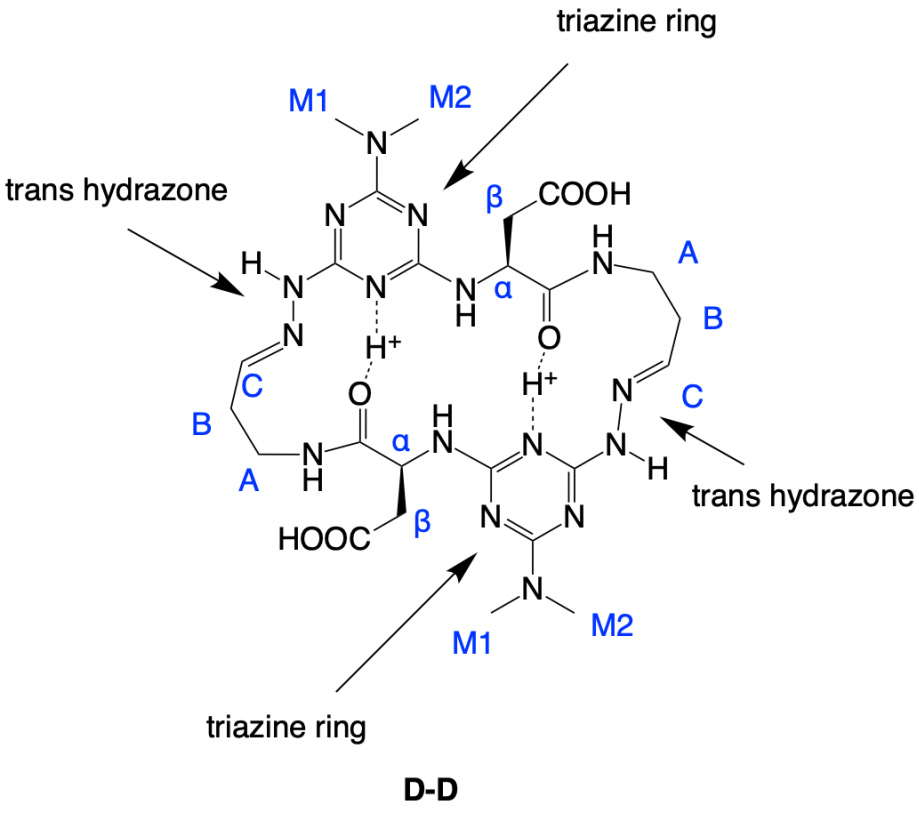

The α-position turns out to be a key determinant of conformation and structure. Having multiple α-signals or splitting show up in the ^{1}H-NMR data can be a sign of what the molecule is doing with regard to its three-dimensional structure.

Another key component is the carbon chain followed by the *trans*-hydrazone. The *trans*-hydrazone is an important factor in conformation of a cyclic structure. The geometry can be determined by looking to see what signals the hydrazone hydrogen interacts with using two-dimensional ^{1}H-NMR. The carbons labeled A-C come from the addition of the acetal. Using a longer chain amino acetal would theoretically lead to a bigger cyclical structure.

Part 2. The Synthesis.

The synthetic route used to prepare the macrocycle is shown in Scheme 1. It starts with stepwise substitution of each chlorine on the triazine ring. By using TLC to monitor the reaction, we found that utilizing a single reaction vessel proved to be an effective strategy. The first substitution involved using a Boc-hydrazine group (blue). The Boc group is especially important because it prevents the hydrazine from reacting early in the synthesis and it can be removed in the last step when TFA is added to cyclize the ring. The dichlorotriazine intermediate (labeled **DCT**) is not isolated, but instead reacted further by adding aspartic acid (red) to yield the monochlorotriazine intermediate, **MCT**, which is not isolated; and then finally, dimethylamine (purple) is added. Dimethylamine (DMA) was chosen as the auxiliary group due to the simplicity it provides in the NMR spectra (two sharp singlets) and its known substitution efficiency. Following extraction and

isolation, we find that **D-acid** can be prepared in a near quantitative yield. Obtaining a quality yield proved critical due to the inefficiency of the acetal reaction.

Scheme 1. Synthesis Route

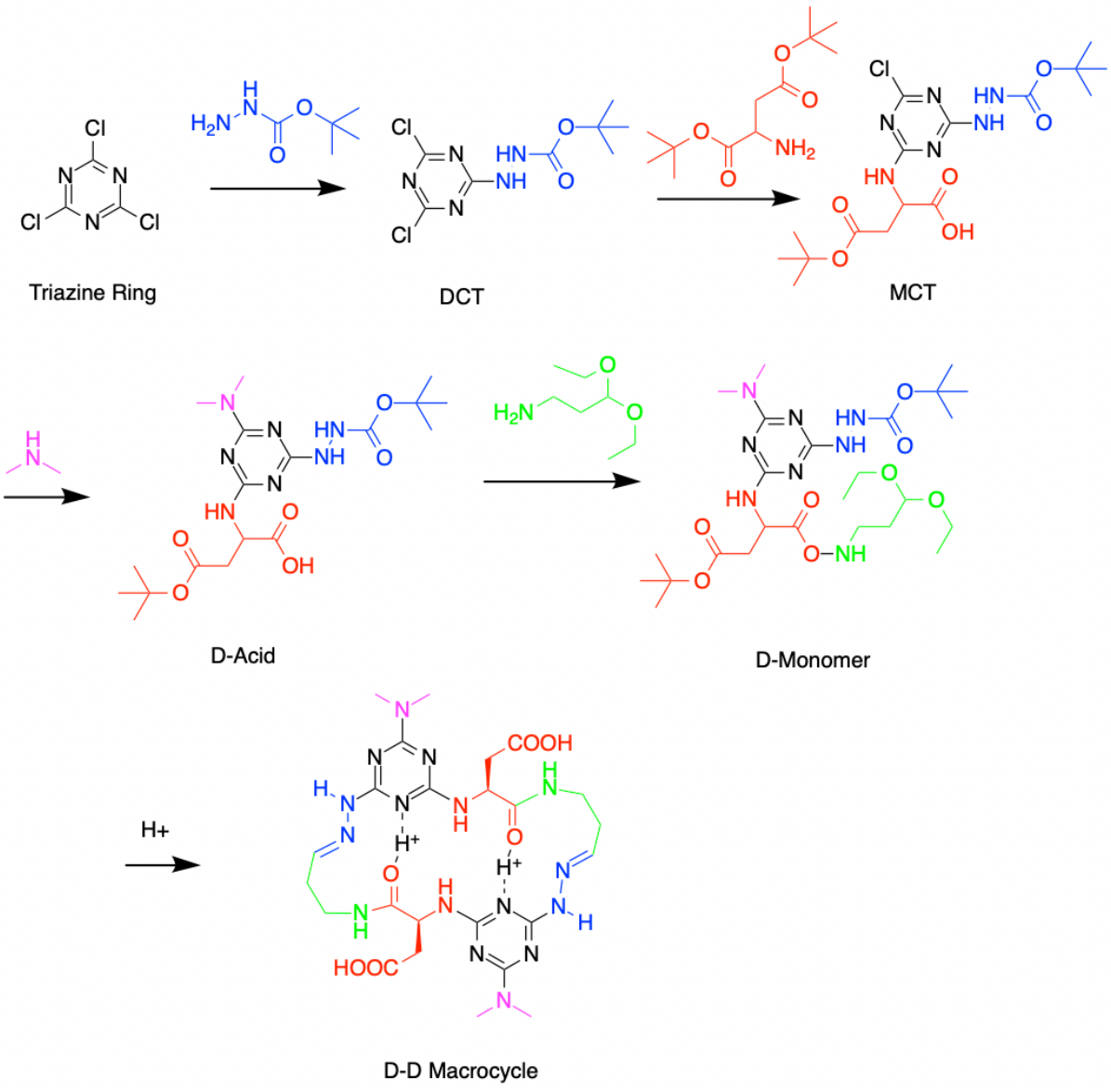

The acetal—a highly reactive aldehyde equivalent— chosen has a three-carbon chain linker. This acetal and the protected hydrazine will eventually undergo condensation to form the hydrazones. Optimization of this reaction is the key step in obtaining a high overall yield. Currently, the yields for this reaction are problematic, but this challenge is not insurmountable. This reaction was first followed using TLC which shows the disappearance of a spot at R_f of 0.3 and appearance of a spot at 0.6 under UV light in 5% MeOH: DCM. This observation confirms that the product formed is less polar than the reactant as expected. When looking at the structure of the product formed, this makes sense because the amine on the acetal attacks the polar carboxylic acid to form an amide.

The final step is the acid-catalyzed dimerization reaction that occurs in 100% yield. Adding a strong acid such as trifluoroacetic acid (TFA) will cleave the pH sensitive BOC group leading to dimerization. To accomplish the reaction, a 1:1 mixture of solvent and TFA is left to evaporate in an uncapped vessel. Using such a strong acid would potentially cause the reaction vessel's cap to melt into the mixture. To obtain a pure compound, the most effective strategy proved to be patiently cyclizing with no cap on the reaction vessel.

Part 3. Characterization of D-Acid and D-Monomer

*Characterization of **D-Acid**.*

As previously stated, the acid intermediate is synthesized via three consecutive additions in a single flask. Each step involves adding a new nucleophile to the reaction mixture to attack one of the electron deficient carbons to produce an equivalent of HCl. The proton is picked up by the addition of base at each step to ensure the chloride atom does not act as a nucleophile itself and

attack the compound being synthesized. The pH of the reaction mixture is essential to maintain due to the Boc group and the protecting t-butyl group on the aspartate both being cleaved if too acidic as well as the formation of additional side products if too basic. The product observed was a single spot by TLC, but indeed needed to be purified via chromatography as a result of various impurities observed in the ^{1}H-NMR spectrum of the crude product.

The precursors to the macrocycle were characterized by NMR spectroscopy which reports on the number of and environments for both protons and carbon atoms within the molecule. The ^{1}H NMR Spectrum of **D-Acid** is shown in Figure 2.

Figure 2: ^{1}H-NMR of Compound 1 in DMSO-*d*$_6$.

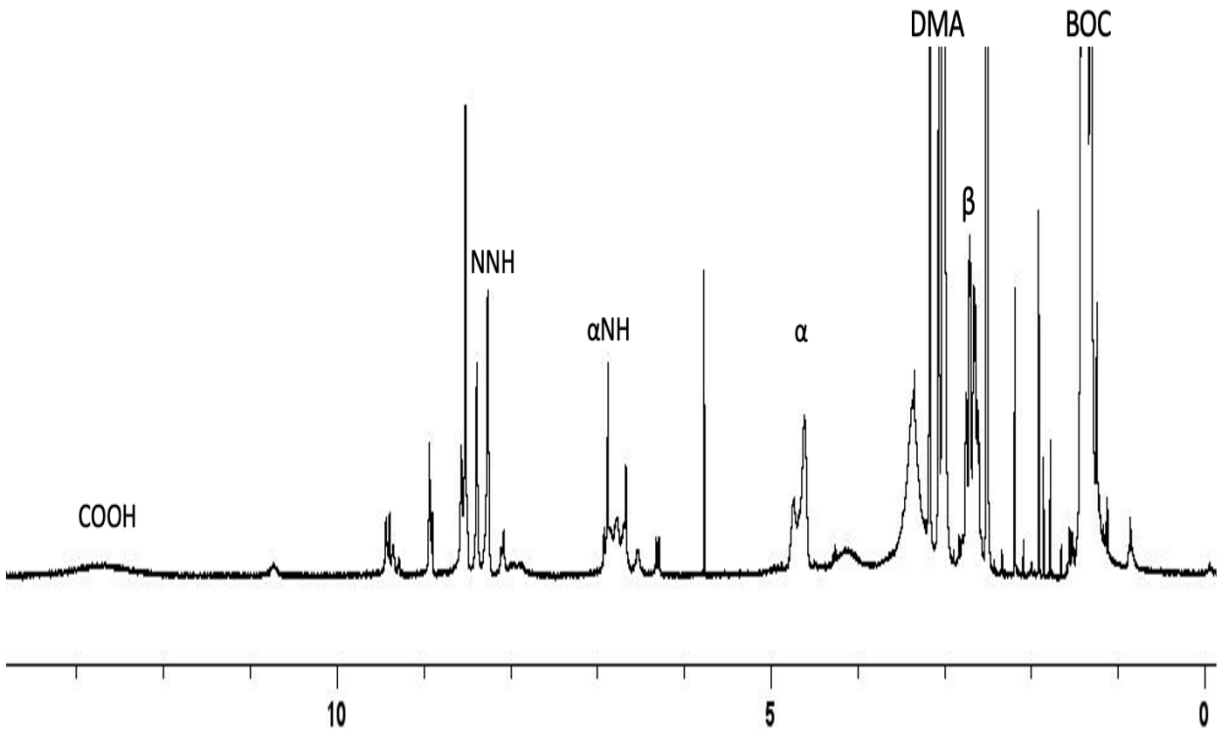

The ^{1}H-NMR spectrum shows critical resonances that ensure that all three substitution reactions occurred on the triazine ring. First, the addition of the DMA group is evident by the two singlets at 3.02 ppm. These methyl groups are different because they sense different environments. In theory, these resonances should integrate to six protons, however in practice we frequently see under integration. Another key feature to suggest successful synthesis of **D-acid** are the α–H resonances for protons at 4.61- 4.73 ppm. This resonance appears as more than one peak because of hindered rotation about the triazine-N bond. Finally, the multiplet at 1.24- 1.56 ppm confirms the addition of both the Boc-hydrazine and the aspartic acid since they are both protected by *t*-butyl groups. While these resonances over-integrate to 24.75, it does confirm that the supposed 18 hydrogens (9 from each protecting group) have been added to the molecule. These groups having been added, along with conformation of DMA addition, means that all three chlorine atoms have been replaced with targeted substituents. Conformation of all three respective groups on the triazine ring without cleaving the protection groups allows for continuation into phase two of the synthesis involving the acetal addition.

*Characterization of **D-Monomer**.*

The length of the acetal carbon chain leads directly to how many atoms will be included in the fully cyclized macrocycle. In this case, a three-carbon chain was utilized in the acetal. It is important the fully cyclized macrocycle has an even number of atoms in the ring because the ultimate product will be a dimer that is symmetrical. Without this, there is significantly more instability associated with the structure.

The ^{1}H NMR spectrum of the monomer is shown in Figure 3 contains a few important things to note. First is the addition of the ethyl acetal chains. The hydrogens bonded to the "B" carbon appear around 3.07 ppm. They also integrate for 6 protons as expected. Furthermore, the spectrum still shows the Boc protecting group, the t-butyl ester, and the DMA groups. This suggests that we have been successful in controlling pH because too much acid causes cleavage of some of these groups. With the structure confirmed, the monomer can be dimerized and the macrocycle completed.

Figure 3: ^{1}H-NMR of Compound 2 in $CDCl_3$.

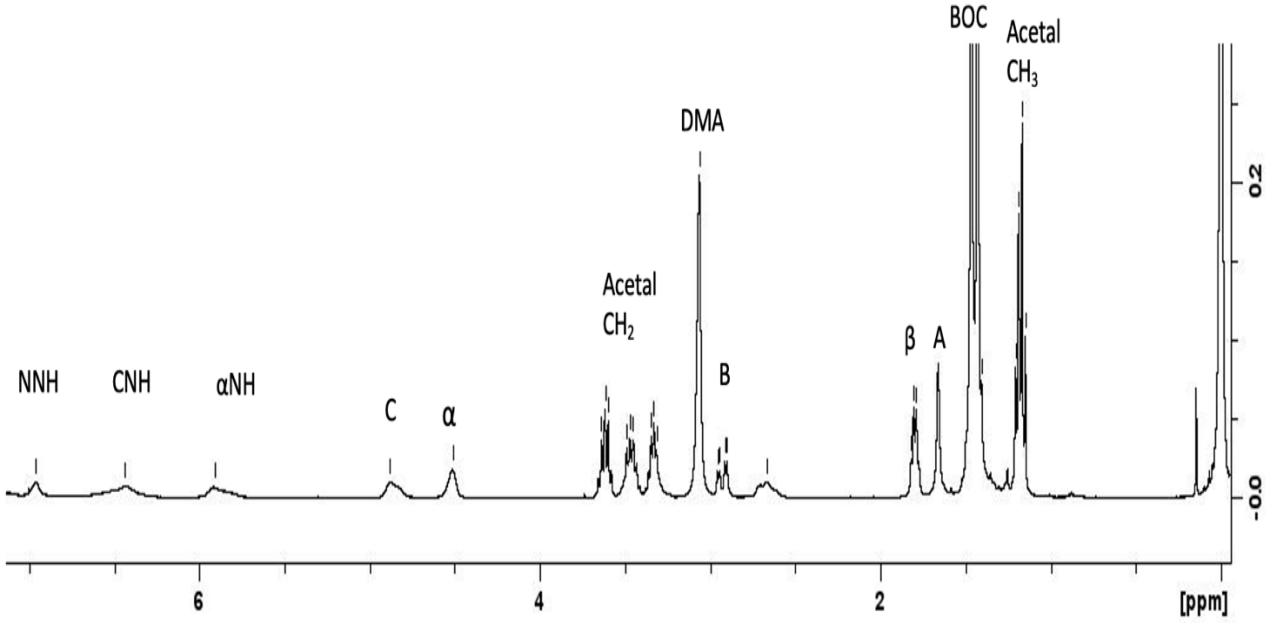

Synthesis of **D-acid** was optimized to a near quantitative yield and the dimerization reaction was observed at a quantitative yield leaving the monomer reaction with the highest risk for product loss. Further optimization of this reaction could lead to significantly better yields for the overall synthesis. Furthermore, the product obtained from the reaction has been observed to decompose slowly if not or kept below room temperature or dimerized within a few hours. Taking all of this into account, the acetal addition is a critical step in the overall synthesis.

Part 4. Synthesis and Characterization of Macrocycle, D-D.

The formation of a homodimer macrocycle occurs when all protecting groups have been cleaved at low pH by adding TFA. TFA removes not only the BOC protecting group and the t-butyl group on the aspartic acid side chain but also catalyzes the formation of the hydrazones. Once all these groups are removed, the molecule is left in a highly reactive state on each end allowing for dimerization with another molecule. Only the macrocycle is produced, and no polymers are observed. The reason for this selectivity is being explored. The ^{1}H NMR spectrum of the macrocycle is shown in Figure 4. It is markedly different than the monomer and acid intermediates.

Figure 4: ^{1}H-NMR of Compound 3 in DMSO-d_6

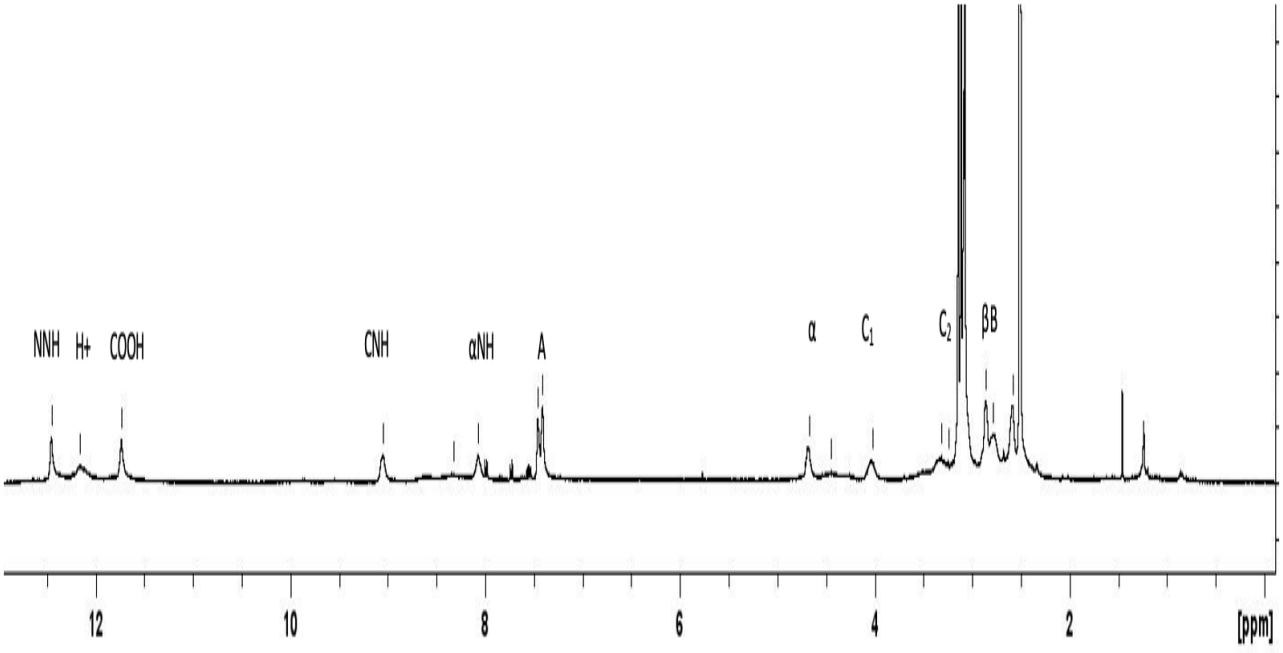

This one-dimensional spectra data strongly supports macrocycle formation, but two-dimensional NMR spectra were necessary for further support of completed structure. These spectra can be analyzed first by looking at the fingerprint region between 13 and 7 ppm to confirm quantitative macrocyclization. The furthest downfield peaks include NNH and COOH peaks at 12.45 ppm and 12.16 ppm, respectively, as well as protonation on the triazine ring at 11.73 ppm. These peaks are observed so far downfield due to the hydrogen atoms being electron deficient and the chemical shift caused by neighboring atoms. Further upfield in the fingerprint region lies hydrogen atom

peaks from CNH, α-NH, and A regions of the macrocycle at 9.05 ppm, 8.07 ppm, 7.46 ppm, respectively. Both NNH and A confirm that the hydrazones have formed.

Moving even further upfield, the resonances observed correspond to hydrogen atoms from the amino acid side chain (4.68 & 2.78-2.86 ppm), carbon chain from the acetal addition (7.41-7.46, 4.45, 5.02, 2.59 ppm), and the DMA (3.07-3.14 ppm) group. Unlike the monomer and the intermediates which showed multiple conformations, there is a single set of resonances for these protons. Many of these peaks are relatively broad suggesting dynamic conformational movement of the macrocycle. Further analysis of the dynamic behavior of the completed macrocycle can be probed with variable temperature NMR studies.

Part 5. Conformational Analysis of the Macrocycle

Many of these resonances were assigned using COSY spectra. This technique proved to be pivotal in three-dimensional shape determination. Figure 5 shows the COSY spectra of the macrocycle. A consecutive array of carbon atoms can be assigned (like A-connected to-B-connected to-C) by looking at the cross peaks that are not on the diagonal. That is, the protons for A and B are on the same horizontal as the two protons of C1 and C2. Similarly, the amino acid protons are all on the same line with α and the two β protons readily assigned. It is important to note that this characterization is through covalent bonds unlike other two-dimensional NMR. This assignment is similar to other macrocyclic compounds synthesized in Simanek's laboratory, suggesting similar shapes. One interesting thing to note is the splitting of the C hydrogens. A number of factors contributed to this determination including integration, COSY interactions, as well as looking at

other molecules. The splitting suggests that the hydrogens are seeing different environments and thus have different chemical shifts.

Figure 5: COSY of Compound 3 in DMSO-*d*$_6$.

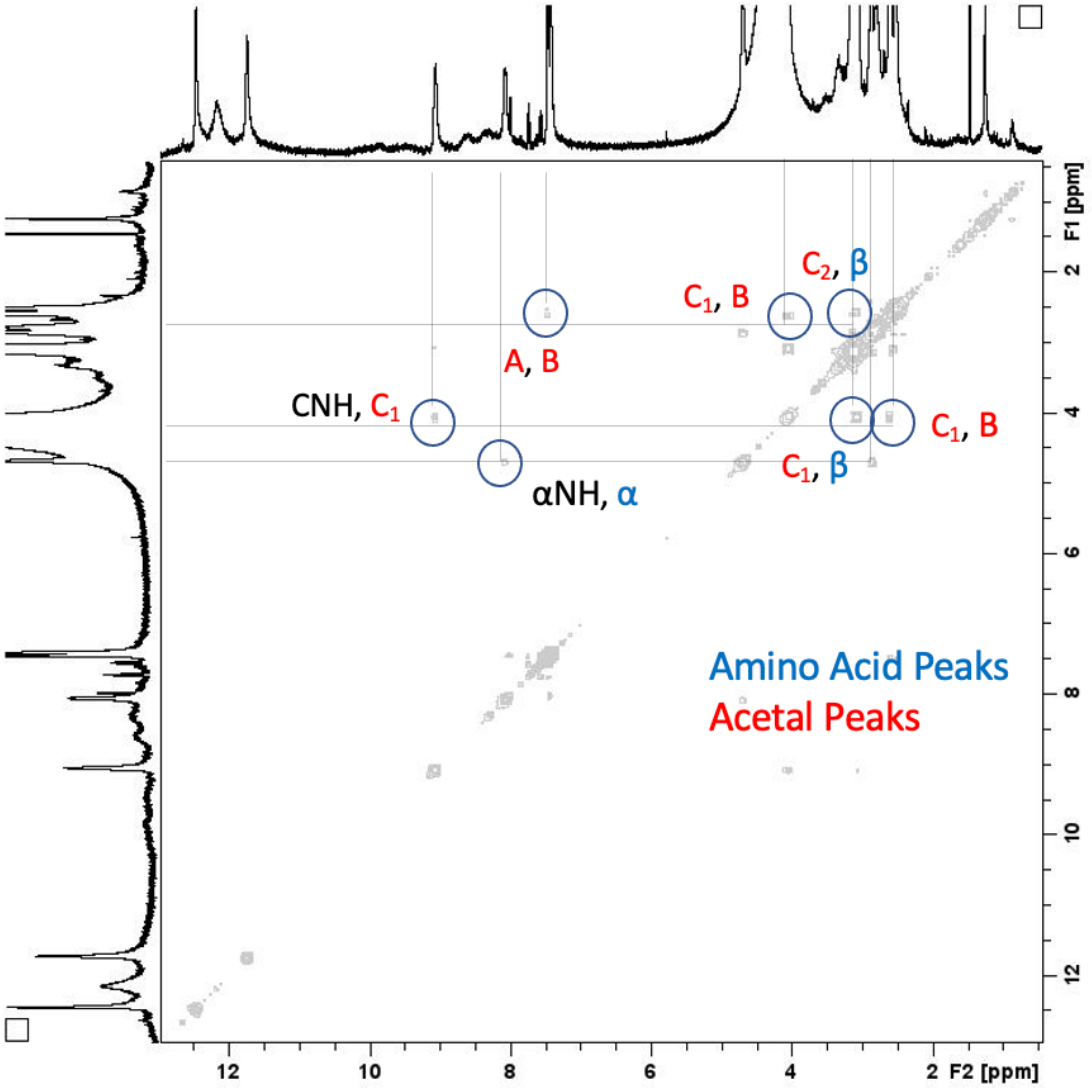

The three-dimensional shape of the molecule is important. To assign shape, we rely on a different NMR experimental technique called ROESY, which reports on interactions through space. From the knowledge of the dynamic behaviors of these molecules, three-dimensional shape could potentially change with different solvents. This ROESY spectrum (see Figure 6) is specifically important in determining if the macrocycle is folded as well as other structural details. For example, the key cross peak for the NNH and A protons region confirms that the hydrazones are in the trans conformation. The strong crosspeak for CNH and α reveals the orientation of the amide bonds. The crosspeak for α-NH and the DMA group confirms that the molecule is folded into a compact structure. In conclusion, the data are very similar to other macrocycles that are known to adopt a folded conformation, although additional work is required including the close proximity of the COOH and A protons.

Figure 6: ROESY of Compound 3 in DMSO-*d*$_6$.

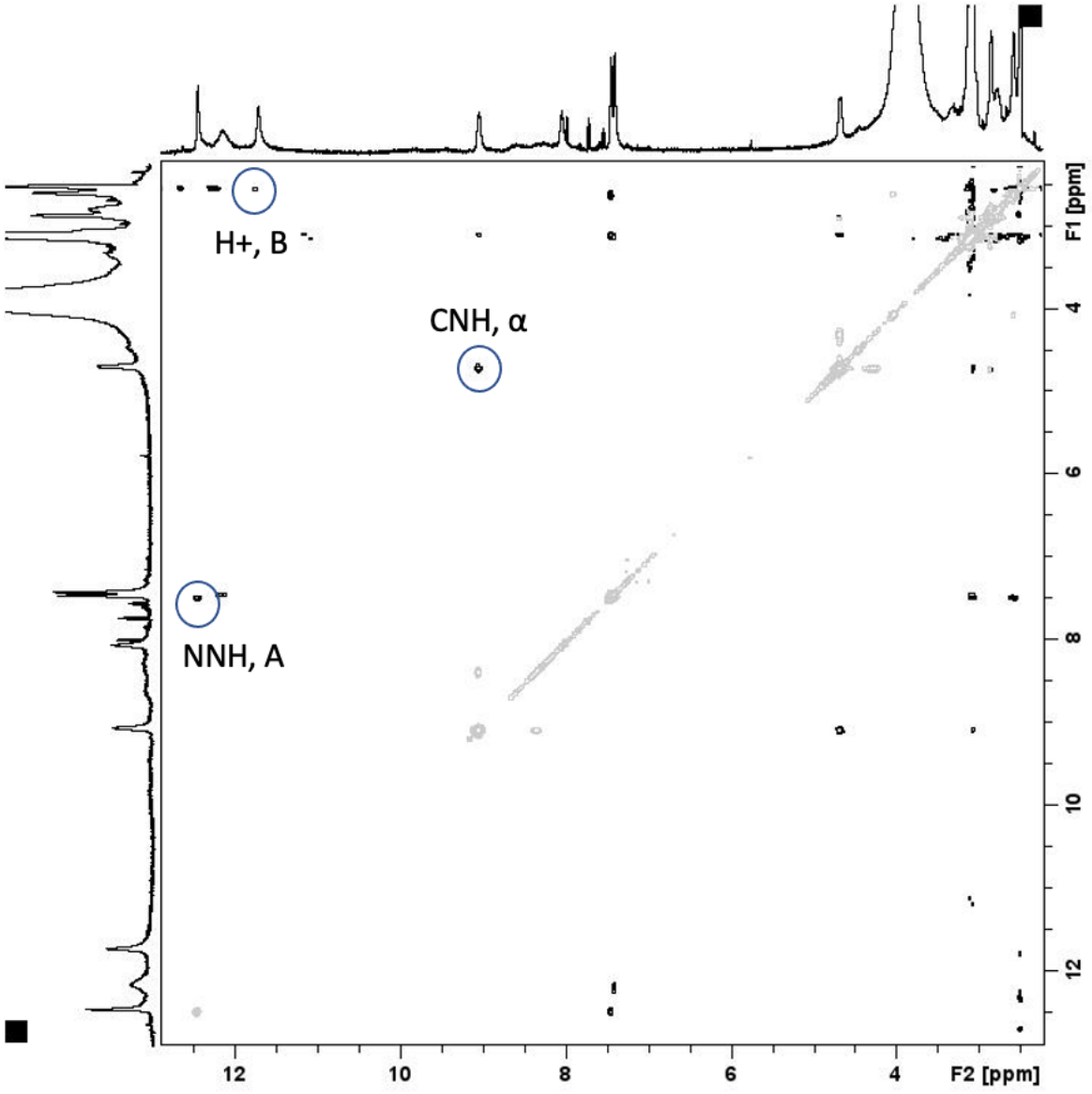

In addition to assigning a static structure of the molecule, understanding its dynamic behavior is very important. One way to probe dynamics is with variable temperature analysis. As the

temperature increases, we expect resonances to merge as they see an averaged chemical environment. Figure 7 shows the stacked one-dimensional ^{1}H NMR spectra of the macrocycle. We would expect that since the alpha hydrogen at room temperature is a single peak that it would continue to do so at the higher temperatures.

Figure 7: Stacked ^{1}H-NMR of Compound 3 in DMSO-d_6 Recorded at Different Temperatures

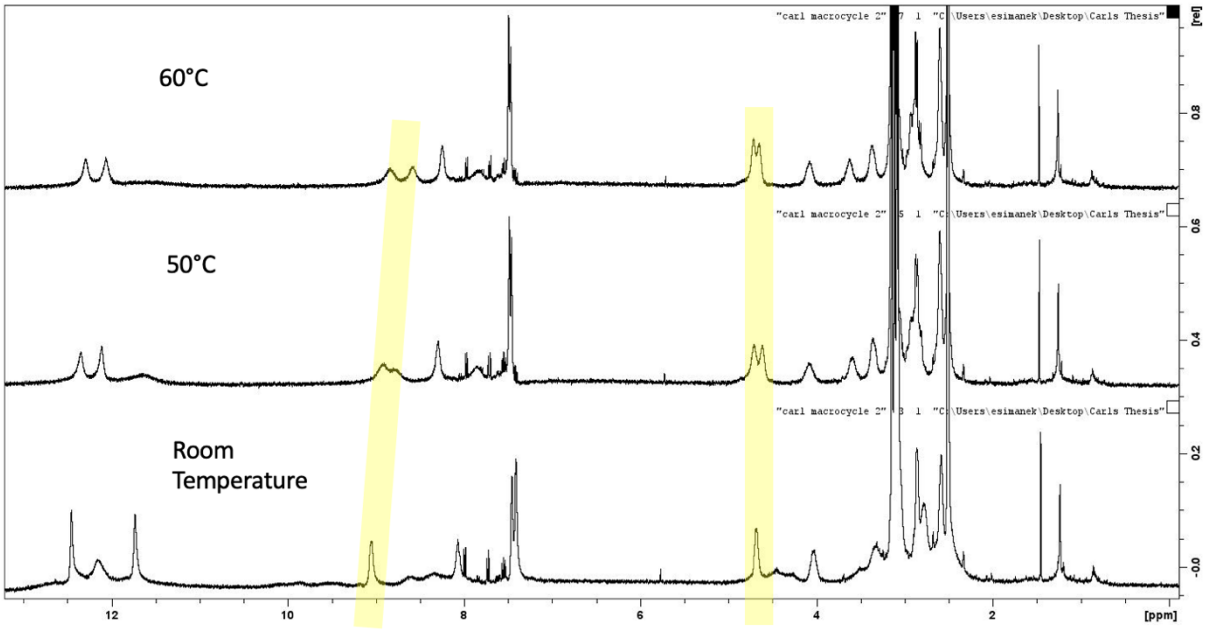

However, we see quite the opposite of what is expected. The α-H splits into two peaks as the temperature is increased from room temperature. A similar behavior is shown by C-NH. It is not clear from the data as to why the molecule is exhibiting this behavior. More analysis in different solvents and further variable temperature analysis is one of the next steps in researching this macrocycle. Determining why the molecule is displaying this specific behavior will serve as a guide to understanding more about this class of molecules.

Conclusion

In summary, the target molecule was synthesized and determined to be relatively pure by TLC data and the NMR spectra. Purity is important in regard to the scope of this research and potential use in pharmaceuticals. Pure material is needed for future experiments including solubility and biological activity. The macrocycle's Log P values will also be measured. These values indicate how soluble a compound is in both lipophilic and hydrophilic environments. According to Lipinski's rule of 5, the best orally available drugs have Log P values below 5. This indicates their ability to be at least partially soluble in various environments. **D-D** will have a varying Log P value since it is pH dependent. These data will be essential to obtain in future determination of biological availability. Still, the study leaves us with more questions than we started with. While the aspartic acid macrocycle was obtained and appears to adopt a conformation similar to other macrocycles, the variable temperature behavior is notably different and puzzling.

The data observed in the synthesis of **D-D** is specifically worthy of interest when looking at the variable temperature data. This class of molecules is studied due to their dynamic nature, and the ^{1}H NMR data conducted at increasing temperature is a prime example of such. The splitting patterns tell a story about the environments that the hydrogens are seeing as the nature of the molecule changes. Further analysis of three-dimensional structure within different environments will be essential in determining macrocycle function. Dynamic nature creates the ability for this one molecule to exhibit numerous functions as the surrounding environment changes– an essential characteristic of oral pharmaceuticals.

References

1. Grigalunas, M.; Burhop, A.; Christoforow, A.; Waldmann, H. Pseudo-Natural Products and Natural Product-Inspired Methods in Chemical Biology and Drug Discovery. *Current Opinion in Chemical Biology*, **2020**, 56, 111–118. DOI: 10.1016/j.cbpa.2019.10.005.
2. Gestwicki, J.; Marinec, P. Chemical Control Over Protein-Protein Interactions: Beyond Inhibitors. *Combinatorial Chemistry & High Throughput Screening*, **2007**, 10, 667–675. DOI: 10.2174/138620707782507296.
3. Wilson, D. L.; Meininger, I.; Strater, Z.; Steiner, S.; Tomlin, F.; Wu, J.; Jamali, H.; Krappmann, D.; Götz, M. G. Synthesis and Evaluation of Macrocyclic Peptide Aldehydes as Potent and Selective Inhibitors of the 20S Proteasome. *ACS Medicinal Chemistry Letters*, **2016**, 7, 250–255. DOI: 10.1021/acsmedchemlett.5b00401.
4. Giordanetto, F.; Kihlberg, J. Macrocyclic Drugs and Clinical Candidates: What Can Medicinal Chemists Learn from Their Properties? *Journal of Medicinal Chemistry*, **2013**, 57, 278–295. DOI: 10.1021/jm400887j.
5. Yepremyan, A.; Mehmood, A.; Asgari, P.; Janesko, B. G.; Simanek, E. E. Synthesis of Macrocycles Derived from Substituted Triazines. *ChemBioChem*, **2018**, 20, 241–246. DOI: 10.1002/cbic.201800475.
6. Vieth, M.; Siegel, M. G.; Higgs, R. E.; Watson, I. A.; Robertson, D. H.; Savin, K. A.; Durst, G. L.; Hipskind, P. A. Characteristic Physical Properties and Structural Fragments of Marketed Oral Drugs. *Journal of Medicinal Chemistry*, **2003**, 47, 224–232. DOI: 10.1021/jm030267j.

7. Sharma, V. R.; Mehmood, A.; Janesko, B. G.; Simanek, E. E. Efficient Syntheses of Macrocycles Ranging from 22–28 Atoms through Spontaneous Dimerization to Yield Bis-Hydrazones. *RSC Advances*, **2020**, 10, 3217–3220. DOI: 10.1039/c9ra08056b.
8. Sillerud, L.; Larson, R. Design and Structure of Peptide and Peptidomimetic Antagonists of Protein- Protein Interaction. *Current Protein & Peptide Science*, **2005**, 6, 151–169. DOI: 10.2174/1389203053545462.
9. Wolfenden, R.; Andersson, L.; Cullis, P. M.; Southgate, C. C. B. Affinities of Amino Acid Side Chains for Solvent Water. *Biochemistry*, **1981**, 20, 849–855. DOI: 10.1021/bi00507a030.